Biochemical and Biophysical Research Communications 455 (2014) 262–268

Contents lists available at ScienceDirect

Biochemical and Biophysical Research Communications

journal homepage: www.elsevier.com/locate/ybbrc

COH-203, a novel microtubule inhibitor, exhibits potent anti-tumor activity via p53-dependent senescence in hepatocellular carcinoma

Huan Qi [a], Dai-Ying Zuo [a], Zhao-Shi Bai [a], Jing-Wen Xu [a], Zeng-Qiang Li [a], Qi-Rong Shen [b], Zhi-Wei Wang [b], Wei-Ge Zhang [b,*], Ying-Liang Wu [a,*]

[a] Department of Pharmacology, Shenyang Pharmaceutical University, Shenyang, China
[b] Key Laboratory of Structure-Based Drug Design and Discovery, Ministry of Education, Shenyang Pharmaceutical University, Shenyang, China

ARTICLE INFO

Article history:
Received 26 October 2014
Available online 6 November 2014

Keywords:
COH-203
Hepatocellular carcinoma
Microtubules
Senescence
p53

ABSTRACT

5-(3-Hydroxy-4-methoxyphenyl)-4-(3,4,5-trimethoxyphenyl)-3*H*-1,2-dithiol-3-one (COH-203) is a novel synthesized analogue of combretastatin A-4 that can be classified as a microtubule inhibitor. In this study, we evaluated the anti-hepatoma effect of COH-203 *in vitro* and *in vivo* and explored the underlying molecular mechanisms. COH-203 was shown to be more effective in inhibiting the proliferation of liver cancer cells compared with normal liver cells. COH-203 also displayed potent anti-tumor activity in a hepatocellular carcinoma xenograft model without significant toxicity. Mechanistic studies demonstrated that treatment with COH-203 induced mitotic arrest by inhibiting tubulin polymerization in BEL-7402 liver cancer cells. Long-term COH-203 treatment in BEL-7402 cells led to mitotic slippage followed by senescence via the $p14^{Arf}$–p53–p21 and $p16^{INK4\alpha}$–Rb pathways. Furthermore, suppression of p53 via pifithrin-α (p53 inhibitor) and p53-siRNA attenuated COH-203-induced senescence in BEL-7402 cells, suggesting that COH-203 induced senescence p53-dependently. In conclusion, we report for the first time that COH-203, one compound in the combretastatin family, promotes anti-proliferative activity through the induction of p-53 dependent senescence. Our findings will provide a molecular rationale for the development of COH-203 as a promising anti-tumor agent.

1. Introduction

Hepatocellular carcinoma (HCC) is the sixth most widespread human tumor and the third leading cause of cancer-related deaths worldwide [1]. Despite great advances in potentially curative treatment modalities for HCC, patient prognosis remains quite poor due to high incidence of recurrence, shortage of liver grafts and frequent resistance [2]. Recently, several studies have demonstrated that the process of microtubule-related cellular assembly represents a crucial step in the development of HCC [3,4], reinforcing that microtubules are likely to serve as an important therapeutic target in HCC. Therefore, it is necessary to discover novel microtubule-targeted agents that display high efficacy and low toxicity for the treatment of HCC.

Combretastatin A-4 (CA-4), a natural *cis*-stilbene product isolated from the South African willow *Combretum caffrum*, has been found to strongly inhibit tubulin polymerization by binding to the colchicine site and exhibits potent anti-cancer activity against a wide variety of cancer cell lines, including multi-drug resistant cell lines [5]. Numerous structure–activity relationship (SAR) studies have confirmed that the *cis*-configuration between the diaryl groups is essential for the strong anti-cancer activities exerted by CA-4 [6]. Oltipraz (OPZ), a synthetic derivative of the naturally occurring dithiolethiones found in cruciferous vegetables, is currently being evaluated in clinical studies as a chemo-protective agent for hepatocarcinogenesis [7]. Hence, a series of novel CA-4/OPZ hybrids with stable *cis*-configuration were synthesized, some of which have been screened for their anti-tumor activities. Among these compounds, COH-203 (5-(3-hydroxy-4-methoxyphenyl)-4-(3,4,5-trimethoxyphenyl)-3*H*-1,2-dithiol-3-one) (CN101429190 B, shown as Fig. 1A) was shown to exhibit the strongest anti-proliferative activity against a wide spectrum of human cancer cell lines, as well as increased stability and bioavailability compared with the parent compound CA-4 (data not shown). However, the definite effect of COH-203 on HCC and the underlying mechanism still remain to be elucidated.

* Corresponding authors at: Department of Pharmacology, Shenyang Pharmaceutical University, 103 Wenhua Road, Shenhe District, Shenyang 110016, China. Fax: +86 24 23986278 (Y.-L. Wu). Key Laboratory of Structure-Based Drug Design and Discovery, Ministry of Education, 103 Wenhua Road, Shenhe District, Shenyang 110016, China. Fax: +86 24 23986393 (W.-G. Zhang).

E-mail addresses: zhangweige2000@sina.com (W.-G. Zhang), yingliang_1016@163.com (Y.-L. Wu).

http://dx.doi.org/10.1016/j.bbrc.2014.11.001
0006-291X/

This study aims to investigate the anti-hepatoma effect and further explore the underlying molecular mechanisms of COH-203 against HCC, which will provide a theoretical basis for developing new promising anti-tumor agents. We demonstrated that COH-203 exhibited potent anti-tumor activity by inhibiting microtubule polymerization, arresting cells at mitosis phase and triggering senescence via p53-dependent pathways.

2. Materials and methods

2.1. Cells and materials

Human HCC cells HepG2, SMMC-7721, BEL-7402 and human normal liver cells HL-7702 were purchased from Shanghai Institute of Cell Resource Center of Life Science (Shanghai, China). All cells were cultured in RPMI-1640 medium (Invitrogen, USA) supplemented with 10% fetal bovine serum (FBS; Hyclone, USA), streptomycin and penicillin at 37 °C in humidified atmosphere with 5% CO_2.

COH-203 and CA-4 were synthesized by our group and the identity and purity (⩾98%) were verified by proton nuclear magnetic resonance and mass spectrometry. For *in vitro* studies, COH-203 and CA-4 were dissolved in dimethyl sulfoxide (DMSO). For animal experiments, the vehicle consisted of 5% ethanol, 20% PEG-400 and 75% saline.

2.2. Cell viability assay

Cells were seeded in 96-well plates with 3000–10,000 cells/well and exposed to various concentrations of COH-203 for the indicated time periods. Cell viability was measured by MTT assay as described previously [8].

2.3. Colony formation assay

BEL-7402 cells were seeded into six-well plates at 1000 cells/well and exposed to COH-203 for 48 h. COH-203 was then removed and fresh medium was replaced every other day. Seven days after COH-203 withdrawal, cells were fixed with 4% paraformaldehyde and stained with crystal violet (1%; Sigma–Aldrich, MO, USA) for 15 min. Colonies were counted visually in each well and photographed using a Canon digital camera.

2.4. Anti-tumor effects in vivo

All animal experimental procedures were performed in accordance with the guidelines of the Animal Experimental Ethics Committee of Shenyang Pharmaceutical University. BEL-7402 cells (4×10^6 cells/nude mice) were injected subcutaneously into the right flank of male 5-week-old BALB/c nude mice. The tumor diameters were measured with digital caliper every 2 days and the volumes were calculated using the formula: (length × width^2)/2. Once tumor volumes reached 200 mm^3, mice were randomized into five treatment groups ($n = 8$) that received: model (vehicle), CA-4 (50 mg/kg) and COH-203 (25, 50 and 100 mg/kg). Treatments were given by intraperitoneal injection every 2 days. By the end of the experiment, all tumor xenografts and organs were removed and measured.

2.5. Tubulin polymerization assay

Cell-free tubulin polymerization assays were performed using the Tubulin Polymerization Assay Kit (Cat.#BK011P; Cytoskeleton, CO, USA) according to the manufacturer's protocol. Briefly, 5 μl of 10 × COH-203, CA-4 or paclitaxel was added to 50 μl of tubulin solution and immediately subjected for kinetic reading using a

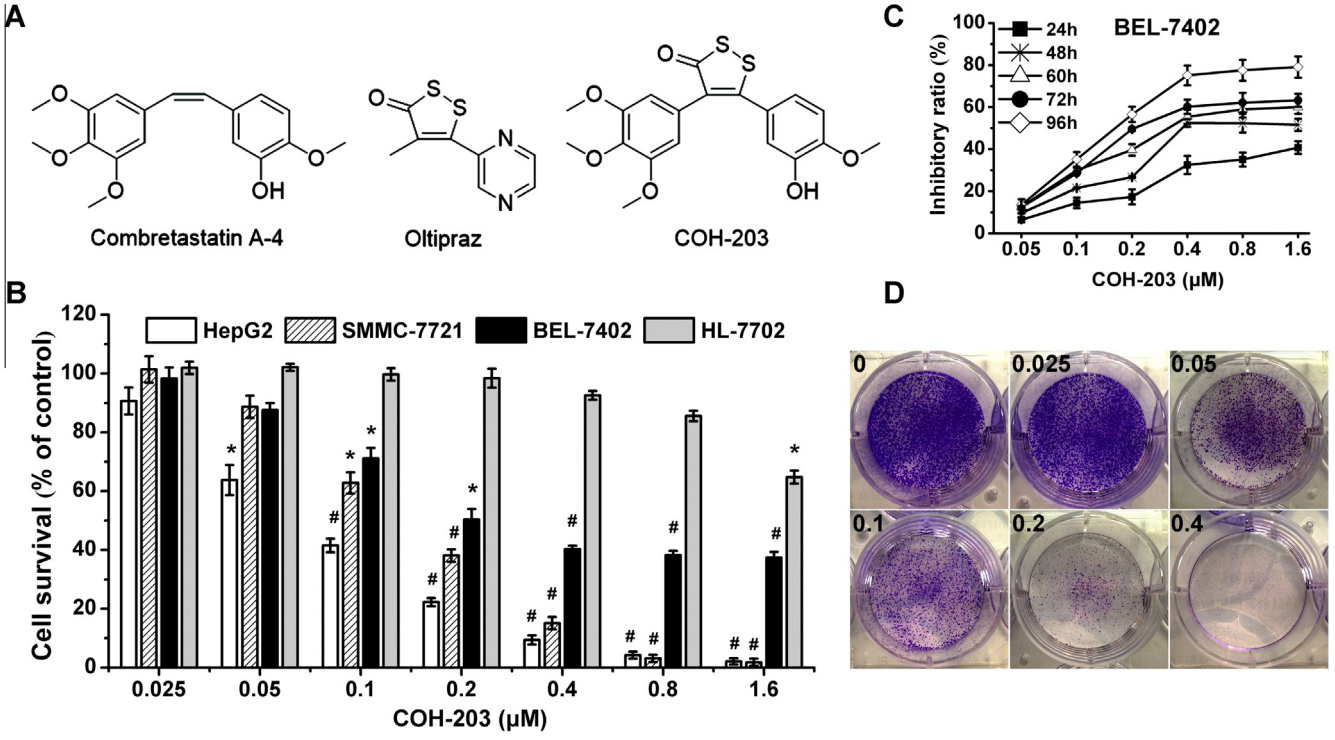

Fig. 1. COH-203 inhibits the proliferation of HCC cells. (A) The chemical structure of CA-4, Oltipraz and COH-203. (B) Dose–responses of three HCC cells and normal liver cells HL-7702 after treatment with COH-203 for 72 h were measured by MTT assay. (C) Cell viability was determined by MTT assay in BEL-7402 cells treated with COH-203 for 24–96 h. (D) The growth inhibition effects of COH-203 (0–0.4 μM) on BEL-7402 cells were measured by colony formation assay. $^*p < 0.05$, $^\#p < 0.01$ compared with control.

plate reader (Varioskan Flash, Thermo, MA, USA) at 37 °C for 90 min.

Intracellular microtubule was measured by western blot as described previously [9]. Briefly, treated BEL-7402 cells were lysed, and the levels of soluble and polymerized tubulin were determined using α-tubulin antibody.

2.6. Immunofluorescence assay

Morphologic changes of microtubules, F-actin and nuclei were examined by immunofluorescence analysis of monoclonal anti-α-tubulin antibody (1:100), rhodamine phalloidin and DAPI, respectively as described previously [10]. Cells were observed under confocal microscopy (Nikon C2, Tokyo, Japan).

2.7. Cycle cell analysis

BEL-7402 cells were treated with the relevant vehicle or COH-203 for indicated time periods, cell cycle distribution was analyzed by flow cytometry as described previously [11].

2.8. Transient transfection of small interfering RNA (siRNA)

BEL-7402 cells plated in six-well plates were cultured for 24 h in RPMI1640 medium with 10% FBS and were transfected with p53 or negative control siRNAs duplexes (100 pmol/well) synthesized by GenePharma Biotechnology (Shanghai, China) using lipofectamine 2000 according to the manufacturer's protocol [12]. The transfected cells were used for subsequent experiments.

2.9. Senescence detection by β-galactosidase staining

Cells plated in 24-well plates were exposed to COH-203 or pifithrin-α (Sigma–Aldrich, MO, USA) for the indicated time points and senescent cells were detected using the Cellular Senescence Assay Kit (Cell Biolabs, CA, USA) according to the manufacturer's protocol [13]. Senescence-associated β-galactosidase (SA-β-Gal) positive cells were observed and counted under phase contrast microscopy.

2.10. Western blot analysis

Western blot analysis was performed as described previously [11]. The primary and secondary antibodies used in this paper are listed in the legend of Fig. S2.

2.11. Statistical analysis

All statistical analyses were performed by SPSS 16.0 software (Chicago, IL, USA) through one-way analysis of variance (ANOVA). $p < 0.05$ was defined as statistical significance. Data and figures represent the mean ± SD (standard deviation) results from three independent experiments.

3. Results

3.1. COH-203 inhibits HCC cells proliferation with low toxicity in normal liver cells

As shown in Fig. 1B, COH-203 treatment was shown to inhibit the growth of the liver cancer cells lines, HepG2, SMMC-7721and BEL-7402 in a concentration-dependent manner, with IC_{50} values as 0.083 ± 0.011, 0.174 ± 0.021 and 0.215 ± 0.025 μM, respectively. To address whether COH-203 promotes general cytotoxicity, the normal liver cell line, HL-7702, was treated with COH-203 for 72 h and revealed that approximately 90% of HL-7702 cells continued to survive at 0.8 μM, which was much higher than the IC_{50} values of three HCC cell lines (Fig. 1B). These results suggest that COH-203 inhibits proliferation of HCC cells but has less anti-proliferative effect on normal liver cells.

Interestingly, although the growth of BEL-7402 cells was time- and concentration-dependently inhibited, there were still a few survival cells at 96 h of treatment with over 0.4 μM COH-203 (Fig. 1C). However, COH-203 treatment led to a concentration-dependent inhibition of BEL-7402 cell colony formation, with the inhibitory rates up to 91% at 0.4 μM (Fig. 1D), which suggests that the COH-203-treated BEL-7402 cells lose capacity to proliferate. Therefore, in order to elucidate the unusual phenomenon, BEL-7402 cells line was chosen for exploring the anti-proliferative mechanism of COH-203.

3.2. COH-203 exhibits potent anti-tumor effect and low toxicity in vivo

To evaluate the anti-tumor effect of COH-203 *in vivo*, we established a nude mice model bearing inoculated BEL-7402 tumors. Remarkably, mice treated with COH-203 (50 or 100 mg/kg) or CA-4 (50 mg/kg) displayed attenuated tumor growth compared with mice treated with vehicle (Fig. S1A). The weight and overall size of the tumors in the COH-203-treated groups (50 and 100 mg/kg) was significantly lower than that of control group (Fig. S1B and C). Analysis of tumor weights revealed inhibitory rates of 11.03%, 42.18% or 53.27% in mice treated with 25, 50 or 100 mg/kg COH-203, respectively, and a 45.09% inhibitory rate in mice treated with 50 mg/kg CA-4.

Throughout the treatment schedule, overt physical discomfort and average body weight change in COH-203-treated mice were not observed compared with control mice. In contrast, the body weight of CA-4-treated mice was obviously decreased (Fig. S1D). Importantly, according to the viscera index analysis (weight of organs (mg)/weight of mice (g)), no differences were observed in the heart, liver, spleen, lung, kidney or brain of the COH-203-treated mice compared with control mice (Fig. S1E).

3.3. COH-203 disrupts tubulin polymerization

To investigate whether COH-203 inhibits microtubule polymerization, the cell-free tubulin polymerization assay was performed to assess microtubule assembly *in vitro*. As shown in Fig. 2A, COH-203 inhibited tubulin polymerization in a concentration-dependent manner compared with control sample. As expected, treatment with CA-4 or paclitaxel was shown to inhibit or enhance tubulin polymerization, respectively.

To further evaluate the effect of COH-203 on microtubule assembly dynamics, we also determined cellular tubulin levels. As shown in Fig. 2B, COH-203 exposure in BEL-7402 cells for 24 h caused a concentration-dependent increase in the proportion of depolymerized (soluble) form to polymerized (insoluble) form of tubulin. Cells treated with CA-4 for 24 h also showed an increase in the depolymerized form of tubulin. Moreover, tubulin immunofluorescence analysis in Fig. 2C revealed that COH-203 treatment for 24 h led to the appearance of astral microtubules surrounded by multiple micronuclei and scattered microtubule fragments in the cytoplasm of BEL-7402 cells, whereas it had no obvious effect on actin cytoskeleton. Together, these findings demonstrated that at both molecular and cellular levels, microtubule assembly was disrupted by COH-203, suggesting the potential tubulin-targeting activity possessed by this agent.

3.4. COH-203 induces mitotic arrest followed by mitotic slippage in BEL-7402 cells

To investigate the effect of COH-203 on cell cycle progression, BEL-7402 cells were treated with different concentrations of

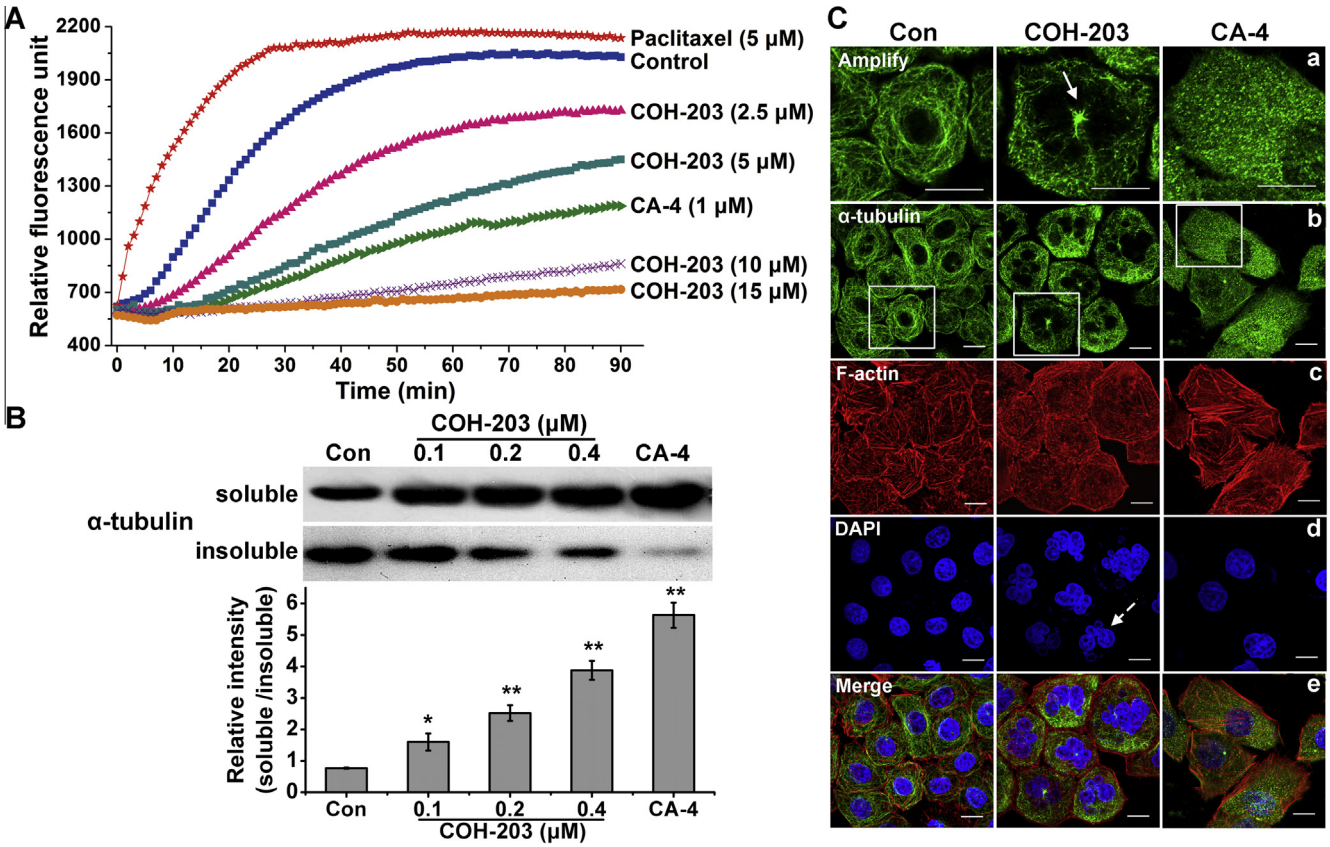

Fig. 2. COH-203 inhibited microtubule polymerization. (A) The effects of various concentrations of COH-203 on microtubules polymerization were evaluated by cell-free tubulin polymerization assay. Paclitaxel and CA4 were used as negative and positive controls, respectively. (B) The levels of polymerized and depolymerized tubulin in BEL-7402 cells treated with COH-203 or CA4 (0.05 μM) for 24 h were detected by western blot. The histogram indicated the relative band intensity between soluble (depolymerized) and insoluble (polymerized) tubulin fractions on arbitrary densitometric units. (C) Changes of cytoskeleton organization were observed by confocal microscopy in BEL-7402 cells treated with COH-203 (0.4 μM) or CA4 (0.03 μM) for 24 h. Microtubules were labeled with a primary mouse anti-α-tubulin antibody and FITC-conjugated goat anti-mouse IgG (green, b); actin filaments were stained with rhodamine-phalloidin (red, c) and the nuclei were stained with DAPI (blue, d). The merged image was shown in e, and the *boxed areas* in b were shown at higher magnification in (a) to illustrate microtubule details. *Solid arrows*, abnormal mitotic spindle and disrupted microtubule networks; *dashed arrows*, multiple micronuclei of different sizes (scale bar = 8 μm). $^{*}p < 0.05$, $^{**}p < 0.01$ compared with control. (For interpretation of the references to color in this figure legend, the reader is referred to the web version of this article.)

COH-203 for 12–72 h and then analyzed by flow cytometry. As shown in Fig. 3A, COH-203 treatment for 24 h promoted a concentration-dependent accumulation of BEL-7402 cells in G2/M phase (up to 80%). To further determine whether the cells arrest specifically in mitosis or G2 phase, p-histone H3 (Ser10), an indicator of mitotic progression, was detected by western blot. As shown in Fig. 3B, the expression of phosphorylation of histone H3 was stimulated a dramatic increase after exposure to COH-203 for 24 h. Immunoblotting also showed that mitosis was triggered between 0 and 24 h of COH-203 treatment as evidenced by accumulation of cyclinB1, and reduction of p-cdc25c (Ser216) and p-cdc2 (Thr14/Tyr15) which negatively regulate the activation of the cyclinB1-cdc2 complex (Fig. 3B). These findings indicate that treatment of BEL-7402 cells with COH-203 induces an arrest in mitosis, but not in G2 phase.

Subsequently, prolonged treatment of BEL-7402 cells with COH-203 led to a substantial increase in the percentage of polyploidy cells (>4 N DNA, up to 65%) between 36 and 60 h and only a small portion of sub-G1 cells (30%) after 72 h (Fig. 3A). Previous studies indicate that multi-nucleated cells arise as a result of abnormal exit from a prolonged mitotic arrest due to cyclinB1 depletion [14,15]. Therefore, to examine whether mitotic slippage is responsible for driving the multi-nucleated phenotype observed in BEL7402 cells, the expression of cell cycle-related proteins was analyzed by western blot after COH-203 (0.4 μM) treatment for 24–72 h. As shown in Fig. 3B, the accumulated cyclinB1 and p-histone H3 (Ser10) at 24 h decreased significantly after 36 h, followed by a transient increase after 48 h and then a permanent declined from 60 h onward. Additionally, this process was negatively regulated by p-cdc2 (Thr14/Tyr15) and p-cdc25c (Ser216). Together, these results suggest that prolonged COH-203-treatment causes BEL-7402 cells to escape from the mitotic arrest without undergoing cytokinesis, enter into the next round of cell cycle, complete DNA replication and may arrest in the following mitotic phase as highly polyploid cells (>4 N).

3.5. COH-203 induces p53-dependent senescence in BEL-7402 cells via $p14^{Arf}$–p53–p21 and $p16^{INK4\alpha}$–Rb pathways

In line with the percentage of sub-G1 cells in Fig. 3A, the results of Annexin V–PI assay also showed that only a small portion (27%) of BEL-7402 cells underwent apoptosis following COH-203 treatment for 72 h (data not shown). However, the fate of the other cells is still unknown. Recently, senescence has been reported to be one fate of the cells suffering from mitotic catastrophe [16]. Hence, we speculated that senescence might be induced in the death process of BEL-7402 cells. As shown in Fig. 4A, COH-203-treated cells exhibited morphological characteristics of senescence such as cell flattening and granulations as well as positive β-galactosidase staining, a hallmark of senescence. The positive SA-β-Gal rate was significantly increased in BEL-7402 cells after 72 h of COH-203 (0.4 μM) treatment and remained high (50%) at 96 h.

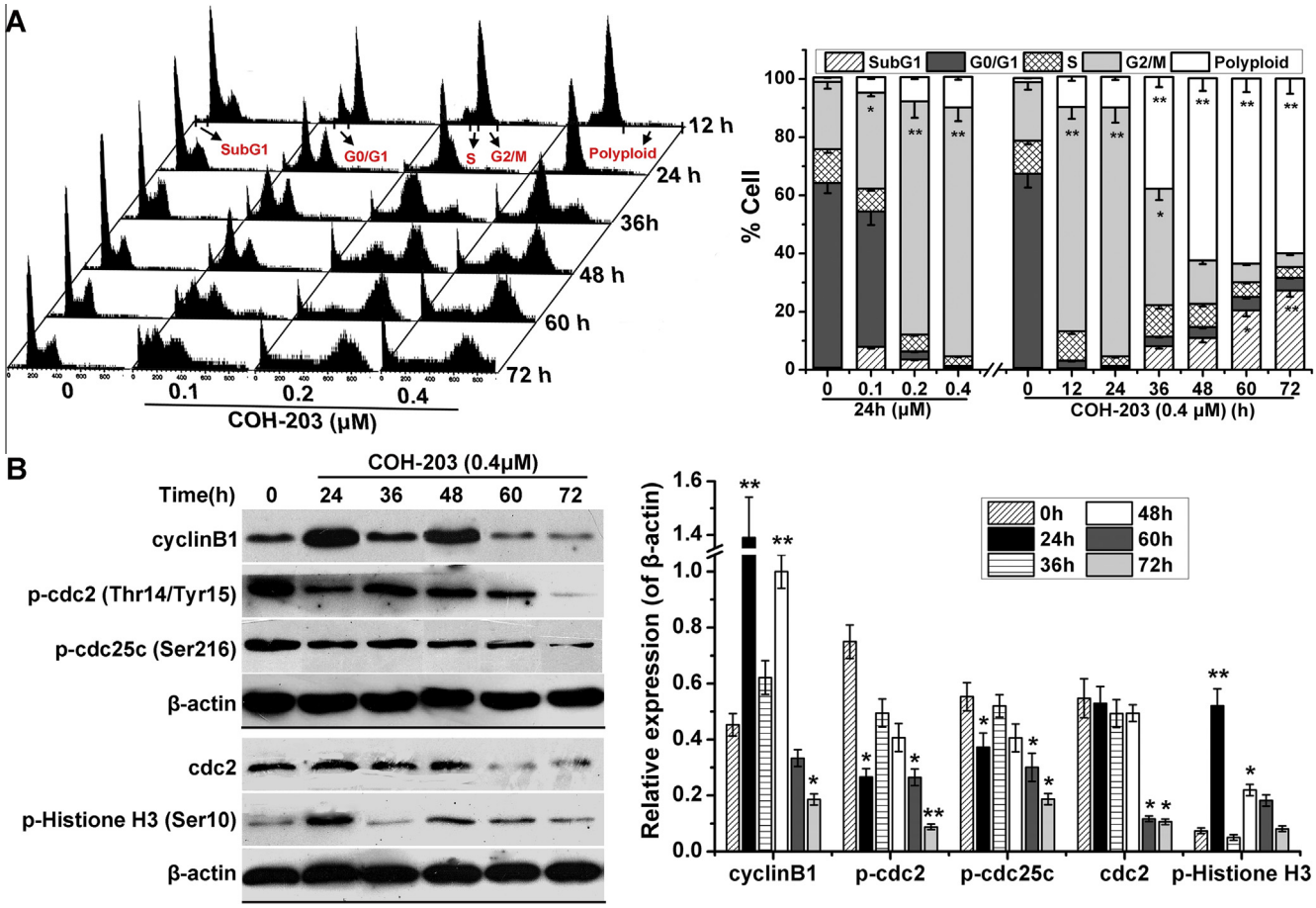

Fig. 3. COH-203 induces mitotic arrest followed by mitotic slippage in BEL-7402 cells. (A) The cell cycle distribution of BEL-7402 cells treated with COH-203 for 12–72 h was measured by flow cytometry with PI staining. Representative figures were shown (left), and the percentage of BEL-7402 cells in specific cell cycle compartments was quantified (right). (B) The expression of G2/M phase-related proteins in BEL-7402 cells treated with COH-203 (0.4 μM) for 0–72 h was analyzed by western blot. The histogram in each panel indicated the relative band intensity ratio generated from three independent experiments. $^{*}p < 0.05$, $^{**}p < 0.01$ compared with control.

It is well established that two classic tumor suppressor pathways, p53–p21 and $p16^{INK4\alpha}$–Rb pathways, are believed to have important contribution in the regulation of cellular senescence, and p53 plays an essential role in this process [17,18]. COH-203 treatment was shown to up-regulate the expression of $p14^{Arf}$, p53, p-p53 and p21 as well as $p16^{INK4\alpha}$ and Rb, whereas expression of an inactive form of Rb, p-Rb, was down-regulated (Figs. 4B and S2A). To further investigate the functional involvement of p53 in COH-203-induced senescence, the p53 inhibitor pifithrin-α and p53-siRNAs were used to suppress p53 function. As shown in Figs. 4C and S2B, p53-siRNA transfection and pifithrin-α reversed the COH-203-induced increase in p53, p21 and Rb protein levels. Moreover, suppression of p53 via chemical or genetic methods attenuated COH-203-induced positive SA-β-Gal staining (Fig. 4D). Together, these results implicate that COH-203 p53-dependently induces senescence in BEL-7402 cells via $p14^{Arf}$–p53–p21 and $p16^{INK4\alpha}$–Rb pathways.

4. Discussion

The results of the present study demonstrate that COH-203, a newly synthesized CA-4/OPZ hybrid with improved stability and bioavailability, exhibits high tumor selectivity to HCC cells *in vitro* and potent anti-tumor effects comparable to CA-4 *in vivo*, with minimal signs of toxicity, suggesting that COH-203 could be considered as a potential therapeutic agent in HCC.

Since it is well known that the parental compound CA-4 is a microtubule inhibitor, we focused the effect of COH-203 on microtubule assembly at molecular and cellular levels. Our data clearly demonstrated that COH-203 inhibited microtubule polymerization in cell-free systems and disrupted the microtubule network in BEL-7402 cells. Our findings also showed that like the other microtubule inhibitors, COH-203 induced mitotic arrest following tubulin de-polymerization. Interestingly, COH-203 treatment induced the formation of multiple micronuclei with various sizes in BEL-7402 cells with 4 N DNA. Previous studies have reported that the formation of micronuclei could result from monopolar, multipolar or disrupted spindles which lead to incomplete sister chromatid segregation during anaphase [19]. Thus, we were encouraged to conclude that COH-203 arrested BEL-7402 cells in mitotic phase by inhibiting microtubule polymerization.

A number of studies have shown that various CA-4-related compounds induce mitotic arrest triggering apoptosis [11,20–22]. In contrast, several reports indicate that cells treated with this class of agents can exit prolonged mitotic arrest without undergoing cytokinesis, enter into next cell cycle and suffer from mitotic catastrophe [23–25]. In this study, after a long exposure to COH-203, BEL-7402 cells escaped from mitotic arrest, entered into the next mitosis as highly polyploid cells, and eventually died via senescence pathways accompanied with a minority of apoptotic cells. During prolonged mitotic arrest, the cell fate is dictated by two competing but independent networks, cell death activation and cyclinB1 degradation. If cyclinB1 levels fall below the

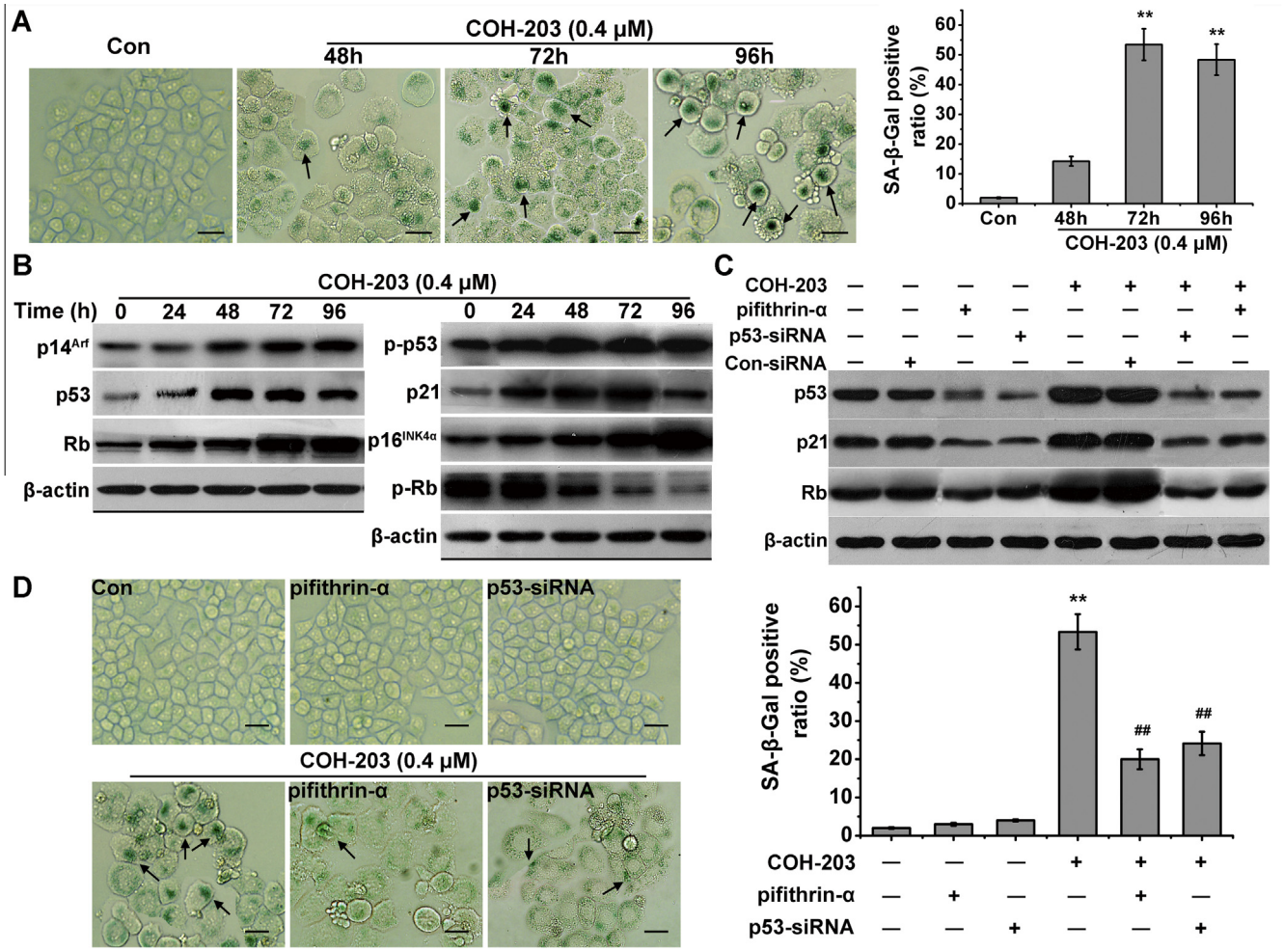

Fig. 4. COH-203 induces p53-dependent senescence in BEL-7402 cells via $p14^{Arf}$–p53–p21 and $p16^{INK4\alpha}$–Rb pathways. (A) Senescence was detected by SA-β-Gal staining after BEL-7402 cells treated with COH-203 (0.4 μM) for 48–96 h. The representative micrograph (left) and the analysis of SA-β-Gal positive ratio (right) were shown (scale bar = 20 μm). (B) The expression of the senescence-associated proteins in BEL-7402 cells treated with COH-203 for 0–96 h was analyzed by western blot. Quantification values are shown in Fig. S2A. (C) The transfected cells or the cells pretreated with pifithrin-α (8 μM) for 3 h were continually incubated with 0.4 μM COH-203 for 72 h, and then the expression of the p53, p21 and Rb proteins was detected by western blot. Quantification values are shown in Fig. S2B. (D) After the transfected or pretreated cells were exposed to COH-203 for 72 h, senescence was detected by SA-β-Gal staining. The representative micrograph (left) and the analysis of SA-β-Gal positive ratio (right) were shown (scale bar = 20 μm). *Black arrows* indicated typical SA-β-Gal positive cells. $^{**}p < 0.01$ compared with control, $^{\#\#}p < 0.01$ compared with COH-203-only treatment group.

threshold of exiting mitosis first, mitotic slippage occurs. If the threshold of cell death is breached first, cell death is triggered [26]. We found that the levels of cyclinB1 decreased significantly in BEL-7402 cells after 36 h of COH-203 treatment and the percentage of multinucleated cells gradually increased, suggesting that mitotic slippage occurred. The detailed mechanism of mitotic slippage as well as the relationship between slippage and apoptosis in COH-203-treated BEL-7402 cells will be further studied.

Cellular senescence is a growth-arrest process to restrain proliferation of tumorigenic cells, and induction of senescence has become an attractive cancer therapeutic strategy [17,27]. To our knowledge, there have also been relatively few studies designed to evaluate the senescence response to microtubule poisons, especially to the compounds in combretastatin family. Here, we demonstrated that long-term (72 h) COH-203 treatment in BEL-7402 cells led to senescence, which was accompanied by gradual activation of $p14^{Arf}$, p53 and p21, followed by increased protein levels of $p16^{INK4\alpha}$ and Rb. These results are quite consistent with the reports that p53 activation and p21 accumulation represent triggers of senescence and that activation of the $p16^{INK4\alpha}$–Rb pathway is involved in maintaining senescence [28,29]. Moreover, we also demonstrated that p53 played a decisive role in COH-203-mediated senescence in BEL-7402 cells. These findings highlight new anti-tumor mechanisms induced by microtubule inhibitors within the combretastatin family.

In summary, our results show that COH-203 exhibits a potent anti-hepatoma effect *in vitro* and *in vivo* with low toxicity. Mechanistically, as a novel synthesized microtubule inhibitor, COH-203 induces mitotic phase arrest, promotes senescence via $p14^{Arf}$–p53–p21 and $p16^{INK4\alpha}$–Rb pathways in HCC cells. Importantly, p53 is demonstrated to be an essential inducer of COH-203-mediated senescence. Taken together, this study reveals a novel mechanism for combretastatin family agents against cancer cells and provides experimental evidence of COH-203 acting as a promising anti-tumor drug.

5. Conflict of interest statement

The authors declare that there are no conflict of interest.

Acknowledgments

The authors would like to thank the National S&T Major Project of China (2012ZX09103101-060), the National Natural Science Foundation of China (30973614) for financial support.

Appendix A. Supplementary data

Supplementary data associated with this article can be found, in the online version, at http://dx.doi.org/10.1016/j.bbrc.2014.11.001.

References

[1] N.N. Rahbari, A. Mehrabi, N.M. Mollberg, et al., Hepatocellular carcinoma: current management and perspectives for the future, Ann. Surg. 253 (2011) 453–469.
[2] T. Livraghi, H. Makisalo, P.D. Line, Treatment options in hepatocellular carcinoma today, Scand. J. Surg. 100 (2011) 22–29.
[3] H.H. Loong, W. Yeo, Microtubule-targeting agents in oncology and therapeutic potential in hepatocellular carcinoma, Onco Targets Ther. 7 (2014) 575–585.
[4] Q. Zhou, A.K. Ching, W.K. Leung, et al., Novel therapeutic potential in targeting microtubules by nanoparticle albumin-bound paclitaxel in hepatocellular carcinoma, Int. J. Oncol. 38 (2011) 721–731.
[5] N.H. Nam, Combretastatin A-4 analogues as antimitotic antitumor agents, Curr. Med. Chem. 10 (2003) 1697–1722.
[6] G.C. Tron, F. Pagliai, E. Del Grosso, et al., Synthesis and cytotoxic evaluation of combretafurazans, J. Med. Chem. 48 (2005) 3260–3268.
[7] R.R. Konwinski, R. Haddad, J.A. Chun, et al., Oltipraz, 3H-1,2-dithiole-3-thione, and sulforaphane induce overlapping and protective antioxidant responses in murine microglial cells, Toxicol. Lett. 153 (2004) 343–355.
[8] F. Qiao, D. Zuo, H. Wang, et al., DAT-230, a novel microtubule inhibitor, induced aberrant mitosis and apoptosis in SGC-7901 cells, Biol. Pharm. Bull. 36 (2013) 193–201.
[9] C.K. Ingemarsdotter, S.K. Baird, C.M. Connell, et al., Low-dose paclitaxel synergizes with oncolytic adenoviruses via mitotic slippage and apoptosis in ovarian cancer, Oncogene 29 (2010) 6051–6063.
[10] Y.Y. Gu, H.Y. Zhang, H.J. Zhang, et al., 8-Chloro-adenosine inhibits growth at least partly by interfering with actin polymerization in cultured human lung cancer cells, Biochem. Pharmacol. 72 (2006) 541–550.
[11] F. Qiao, D. Zuo, X. Shen, et al., DAT-230, a novel microtubule inhibitor, exhibits potent anti-tumor activity by inducing G2/M phase arrest, apoptosis in vitro and perfusion decrease in vivo to HT-1080, Cancer Chemother. Pharmacol. 70 (2012) 259–270.
[12] D.L. Chen, J.N. Xiang, L.Y. Yang, Role of ERp46 in beta-cell lipoapoptosis through endoplasmic reticulum stress pathway as well as the protective effect of exendin-4, Biochem. Biophys. Res. Commun. 426 (2012) 324–329.
[13] M. Qi, S. Fan, G. Yao, et al., Pseudolaric acid B-induced autophagy contributes to senescence via enhancement of ROS generation and mitochondrial dysfunction in murine fibrosarcoma L929 cells, J. Pharmacol. Sci. 121 (2013) 200–211.
[14] D.A. Brito, C.L. Rieder, Mitotic checkpoint slippage in humans occurs via cyclin B destruction in the presence of an active checkpoint, Curr. Biol. 16 (2006) 1194–1200.
[15] I.B. Roninson, E.V. Broude, B.D. Chang, If not apoptosis, then what? Treatment-induced senescence and mitotic catastrophe in tumor cells, Drug Resist. Updat. 4 (2001) 303–313.
[16] I. Vitale, L. Galluzzi, M. Castedo, et al., Mitotic catastrophe: a mechanism for avoiding genomic instability, Nat. Rev. Mol. Cell Biol. 12 (2011) 385–392.
[17] C.A. Schmitt, J.S. Fridman, M. Yang, et al., A senescence program controlled by p53 and p16INK4a contributes to the outcome of cancer therapy, Cell 109 (2002) 335–346.
[18] C. Borlon, S. Vankoningsloo, P. Godard, et al., Identification of p53-dependent genes potentially involved in UVB-mediated premature senescence of human skin fibroblasts using siRNA technology, Mech. Ageing Dev. 129 (2008) 109–119.
[19] J.M. Holy, Curcumin disrupts mitotic spindle structure and induces micronucleation in MCF-7 breast cancer cells, Mutat. Res. 518 (2002) 71–84.
[20] H. Zhu, J. Zhang, N. Xue, et al., Novel combretastatin A-4 derivative XN0502 induces cell cycle arrest and apoptosis in A549 cells, Invest. New Drugs 28 (2010) 493–501.
[21] R. Wu, W. Ding, T. Liu, et al., XN05, a novel synthesized microtubule inhibitor, exhibits potent activity against human carcinoma cells in vitro, Cancer Lett. 285 (2009) 13–22.
[22] S. Bhattacharya, N.M. Kumar, A. Ganguli, et al., NMK-TD-100, a novel microtubule modulating agent, blocks mitosis and induces apoptosis in HeLa cells by binding to tubulin, PLoS One 8 (2013) e76286.
[23] L.M. Greene, N.M. O'Boyle, D.P. Nolan, et al., The vascular targeting agent combretastatin-A4 directly induces autophagy in adenocarcinoma-derived colon cancer cells, Biochem. Pharmacol. 84 (2012) 612–624.
[24] S.M. Nabha, R.M. Mohammad, M.H. Dandashi, et al., Combretastatin-A4 prodrug induces mitotic catastrophe in chronic lymphocytic leukemia cell line independent of caspase activation and poly(ADP-ribose) polymerase cleavage, Clin. Cancer Res. 8 (2002) 2735–2741.
[25] C.H. Shen, J.J. Shee, J.Y. Wu, et al., Combretastatin A-4 inhibits cell growth and metastasis in bladder cancer cells and retards tumour growth in a murine orthotopic bladder tumour model, Br. J. Pharmacol. 160 (2010) 2008–2027.
[26] K.E. Gascoigne, S.S. Taylor, Cancer cells display profound intra- and interline variation following prolonged exposure to antimitotic drugs, Cancer Cell 14 (2008) 111–122.
[27] M.E. Lleonart, A. Artero-Castro, H. Kondoh, Senescence induction; a possible cancer therapy, Mol. Cancer 8 (2009) 3.
[28] G.H. Stein, L.F. Drullinger, A. Soulard, et al., Differential roles for cyclin-dependent kinase inhibitors p21 and p16 in the mechanisms of senescence and differentiation in human fibroblasts, Mol. Cell. Biol. 19 (1999) 2109–2117.
[29] F. Rodier, J. Campisi, Four faces of cellular senescence, J. Cell Biol. 192 (2011) 547–556.